Chinese Medical Journal®

SENP2-mediated SERCA2a deSUMOylation increases calcium overload in cardiomyocytes to aggravate myocardial ischemia/reperfusion injury

Yuanyuan Luo[1], Shuaishuai Zhou[2], Tao Xu[2], Wanling Wu[1], Pingping Shang[2], Shuai Wang[2], Defeng Pan[1], Dongye Li[1,2]

[1]Department of Cardiology, The Affiliated Hospital of Xuzhou Medical University, Xuzhou, Jiangsu 221006, China;
[2]Institute of Cardiovascular Disease Research, Xuzhou Medical University, Xuzhou, Jiangsu 221002, China.

Abstract

Background: Sarcoplasmic reticulum calcium ATPase 2a (SERCA2a) is a key protein that maintains myocardial Ca^{2+} homeostasis. The present study aimed to investigate the mechanism underlying the SERCA2a-SUMOylation (small ubiquitin-like modifier) process after ischemia/reperfusion injury (I/RI) *in vitro* and *in vivo*.

Methods: Calcium transient and systolic/diastolic function of cardiomyocytes isolated from *Serca2a* knockout (KO) and wild-type mice with I/RI were compared. SUMO-relevant protein expression and localization were detected by quantitative real-time PCR (RT-qPCR), Western blotting, and immunofluorescence *in vitro* and *in vivo*. Serca2a-SUMOylation, infarct size, and cardiac function of Senp1 or Senp2 overexpressed/suppressed adenovirus infected cardiomyocytes, were detected by immunoprecipitation, triphenyltetrazolium chloride (TTC)-Evans blue staining, and echocardiography respectively.

Results: The results showed that the changes of Fura-2 fluorescence intensity and contraction amplitude of cardiomyocytes decreased in the I/RI groups and were further reduced in the *Serca2a* KO + I/RI groups. Senp1 and Senp2 messenger ribose nucleic acid (mRNA) and protein expression levels *in vivo* and in cardiomyocytes were highest at 6 h and declined at 12 h after I/RI. However, the highest levels in HL-1 cells were recorded at 12 h. Senp2 expression increased in the cytoplasm, unlike that of Senp1. Inhibition of Senp2 protein reversed the I/RI-induced Serca2a-SUMOylation decline, reduced the infarction area, and improved cardiac function, while inhibition of Senp1 protein could not restore the above indicators.

Conclusion: I/RI activated Senp1 and Senp2 protein expression, which promoted Serca2a-deSUMOylation, while inhibition of Senp2 expression reversed Serca2a-SUMOylation and improved cardiac function.

Keywords: Myocardial ischemia; Reperfusion injury; Sarcoplasmic reticulum calcium-transporting ATPases; Sentrin/SUMO-specific protease; Calcium overload

Introduction

Reducing myocardial damage associated with coronary artery disease is the primary goal in prognostic management.[1,2] Extensive evidence shows that ischemia/reperfusion injury (I/RI) may occur after revascularization. I/RI refers to cardiomyocyte apoptosis and death, which lead to myocardial stunning, no-reflow phenomena, a decline in cardiac function, and death.[3–5] Exploring the mechanism and developing drugs for attenuating cardiac I/RI have become a major focus of research in recent years.[6,7]

Calcium overload is an important mechanism underlying I/RI.[8] Sarcoplasmic reticulum calcium ATPase 2a (SERCA2a) is mainly localized in the sarcoplasmic reticulum and endoplasmic reticulum membrane and accumulates in the T-tube of cardiomyocytes. In human cardiomyocyte cytoplasm, approximately 70% of Ca^{2+} is removed by SERCA2a.[9,10] Previous studies have generally focused on the role of SERCA2a in heart failure, showing that both the activity and level of SERCA2a decline.[11–14] Introducing the *SERCA2A* gene into cardiomyocytes improves cardiac function in cardiomyocytes of animals with heart failure.[11,15] Some clinical trials have used *SERCA2a* transgenic therapy to treat human heart failure.[16,17] In I/RI models, some researchers have reported a reduction in the level of SERCA2a phosphorylation.[18] Reversing the expression or reduction of SERCA2a activity may provide a new pathway to treat cardiomyocyte injury induced by calcium overload.[8,19,20]

Modification by a small ubiquitin-related modifier (SUMO) is a type of post-translational protein modification. The SUMO protein first connects with the E1 kinase and then transfers to the cysteine residue of the

Access this article online

Quick Response Code:

Website: www.cmj.org

DOI: 10.1097/CM9.0000000000002757

Correspondence to: Dongye Li, Institute of Cardiovascular Disease Research, Xuzhou Medical University, 84 West Huaihai Road, Xuzhou, Jiangsu 221002, China
E-Mail: dongyeli@xzhmu.edu.cn

Chinese Medical Journal 2023;136(20)
Received: 01-10-2022; **Online:** 18-07-2023 **Edited by:** Xiuyuan Hao

E2 conjugate. The efficiency and specificity of ubiquitin-conjugating enzyme 9 (UBC9) is enhanced by E3 conjugase. Under the action of the de-SUMOylation enzymes (sentrin/SUMO-specific protease [SENP] or deSUMOylating isopeptidase [DESI]), the SUMO molecule dissociates from the protein and re-enters SUMOylation cycling.[21,22] SUMOylation modification can regulate the expression of SERCA2a at the transcriptional and protein levels.[23] Overexpression of SUMO1 but not SUMO2/3 improves the activity of SERCA2a and cardiac function.[24–26]

SENPs include SENP1–3 and 5–7.[27,28] SENPs are localized at different positions under different pathophysiological conditions and exert different biological effects.[29,30] SUMO1 molecule dissociates from the proteins by the only two deSUMOylation enzymes which are SENP1 and SENP2. Heo *et al*[31] have reported that the spatial locations of SENP1 and SENP2 are regulated via the nuclear export and nuclear localization signals shuttling between the nucleus and the cytoplasm and modified proteins at different sites. Gu *et al*[32] have reported up-regulation of SENP1 in cardiomyocytes following I/RI in humans, mice, and rats. However, the exact mechanism of SENPs in SERCA2a SUMOylation in I/RI pathology is unclear.

The current study utilized *Serca2a*$^{flox/flox}$ Tg (*αMHC-MerCreMer*) mice (*Serca2a* knockout mice [*Serca2a* KO mice]) to observe the effect of Serca2a on calcium overload following I/RI. The reduction mechanism of Serca2a SUMOylation induced by I/RI provides the theoretical and experimental bases for the development of effective drugs against I/RI.

Methods

Materials

The HL-1 cells were donated by Professor Chen Minglong of Nanjing Medical University and authorized by William C. Claycomb from the Department of Biochemistry and Molecular Biology, Louisiana State University, USA. C57BL/6J mice weighing 25–30 g were purchased from Jinan Pengyue Experimental Animal Breeding Co., Ltd. (Xuzhou, China). *Serca2a*$^{flox/flox}$ Tg (*αMHC-MerCreMer*) mice were donated by Professor Ole M. Sejersted of Oslo University Hospital Ulleval. All research was approved by the Animal Ethics Committee of Xuzhou Medical University (No. CMCACUC 2017-04-132).

The pHBAd-U6-Senp1-CMV-RFP (Red fluorescent protein), pHBAd-U6-Senp2-CMV-GFP (Green fluorescent protein), pHBAd-U6-CMV-RFP/GFP, pHBAd-U6-Senp1-shRNA-GFP, and pHBAd-U6-Senp2-shRNA-RFP were constructed by Hanbio Biotechnology Co. Ltd. (Shanghai, China). The short hairpin RNA (shRNA) oligonucleotides were shown in Table 1.

Mouse I/RI model

The mice were fasted for 12 h before being anesthetized with isoflurane. The electrocardiogram was recorded using a BL-420S Biological Signal Processing System (Chengdu Techman Co., Chengdu, China). The ventilator was turned on with the following parameters: tidal volume, 10 mL; excitation/inhibition ratio, 1:2; and respiratory rate, 90 breath/min. The chest was opened along the left midaxillary line and the left anterior descending (LAD) artery was identified. A suture thread was passed below the LAD artery and an empty balloon was placed outside it for ligation. The balloon was pressurized to occlude the LAD artery and then emptied and removed 30 min later.[33]

Table 1: The sequence of shRNA oligonucleotides of *Senp1* and *Senp2*.

Genes	shRNA
Senp1	shRNA1: CGGAAGACCTCAAGTGGATTATCAA
Senp1	shRNA2: AAGCCACCAGCTGACTGACAGTGAA
Senp1	shRNA3: GAAGCCCAGCCTATCGTCCAGATTA
Senp2	shRNA1: GCAGCATGCTGAAACTGGGTAATAA
Senp2	shRNA2: CCTAATGGAATAAGCGACTATCCAA
Senp2	shRNA3: GCGACTTAAAGAAGGTGCTCATGGA

shRNA: Short hairpin ribose nucleic acid.

Cardiomyocyte isolation via the Langendorff system

The mice were anesthetized and the skin was incised below the xiphoid process. The aorta was cut 3 mm below the heart. The heart was infused with a calcium-free solution (NaCl 120 mmol/L, KCl 5.4 mmol/L, $MgSO_4 \cdot 7H_2O$ 1.2 mmol/L, NaH_2PO_4 1.2 mmol/L, $NaHCO_3$ 20 mmol/L, glucose 5.6 mmol/L, 2,3-butadione monoxime (BDM) 10 mmol/L, and taurine 5 mmol/L) for 4 min using a Langendorff system (ThermoFisher, MA, USA), followed by perfusion with an enzyme solution (collagenase 2 0.5 mg/mL, collagenase 4 0.5 mg/mL, protease XIV 0.05 mg/mL [Invitrogen, MA, USA], and 1 μL $CaCl_2$ 1 mol/L) for 5–8 min. Part of the left ventricle was subjected to blowing and suction until the lumps disappeared. The stopping solution (calcium-free solution containing 5% sterile fetal bovine serum, Invitrogen) was then added and calcium recovery was implemented.

Calcium transient and diastolic/systolic function detection of cardiomyocytes

Tamoxifen (8 μg/L; Sigma-Aldrich LLC, Darmstadt, Germany) was intraperitoneally injected into *Serca2a*$^{flox/flox}$ Tg (*αMHC-MerCreMer*) mice.[34] *Serca2a*$^{flox/flox}$ Tg (*αMHC-MerCreMer*) mice were intraperitoneally injected with tamoxifen 1 mg daily for 4 consecutive days, whereas control *Serca2a*$^{flox/flox}$ Tg (*αMHC-MerCreMer*) mice were intraperitoneally injected with the same dose of peanut oil. The *Serca2a* KO efficiency was measured 2 weeks later by quantitative real-time polymerase chain reaction (RT-qPCR) and Western blotting.

Cardiomyocytes were divided into the following groups: wild-type (WT), *Serca2a* KO, I/RI, and *Serca2a* KO + I/RI ($n = 3$). For the I/RI and Serca2a KO + I/RI groups, the pale myocardium below the ligature line of the ante-

rior descending branch to the anterior wall of the apex was harvested. Calcium recovery was performed using a gradient solution to reach a Ca^{2+} concentration of 1.5 mmol/L. The cells were then incubated with 1 μmol/L Fura2-AM (Dojindo Molecular Tech., Inc., Kumamoto, Japan) at 37°C for 20 min. An IonOptix MyoCam system (IonOptix Corporation, Milton, MA, USA) was used to detect the contraction amplitude and contractile/systolic speed of the cardiomyocytes. Changes in the concentration of free Ca^{2+} were characterized by the fluorescence intensity ratio at 340 nm and 380 nm.[35] Ten cardiomyocytes were collected for detection from each group. Transient was measured based on the changes of Fura-2 fluorescence intensity (ΔFFI). Contraction amplitude of cardiomyocytes was measured based on cell length peak height.

HL-1 simulation ischemia /reperfusion injury (sI/RI) model

The culture medium was discarded and Hank's balanced salt solution was added to the cell. The cells were placed into a 3-gas incubator for hypoxia for 1.5 h (1% O_2, 5% CO_2, and 94% N_2). The medium was replaced with a normal medium and 2 h reoxygenation was performed to simulate I/RI, which was followed by cell harvesting.

RT-qPCR

RNA extraction from the tissues/cells was performed with the Trizol reagent (Invitrogen, Carlsbad, USA) and used for generating cDNA (Sangon Biotech Co., Ltd., Shanghai, China) in the presence of oligo-dT primers. RT-qPCR was performed using ready-to-use PCR Real MasterMix (Tiangen Biotech Beijing Co., Beijing, China) with glyceraldehyde 3-phosphate dehydrogenase as the internal control. The primers were shown in Table 2.

Table 2: The primers of mouse *Sumo1*, *Ubc9*, *Senp1*, and *Senp2*.

Genes	Primers
Sumo1	Forward: GAATTATCTAAACCGTCGAGTGAC
	Reverse: AAA GAACTGGGAATGGAGGAA
Ubc9	Forward: TTGAACAAGCCTCCTTCCCAT
	Reverse: CTGTCCCAACAAAGAACCCTG
Senp1	Forward: GCTATTTGGCTGATGAGGTGC
	Reverse: CCTGTCTCGGTGTCTTAGTTCC
Senp2	Forward: TCTGGTGCTGAGTGAATGTGA
	Reverse: GTTGAATGGGAGTGACTGTGG

Western blotting and co-immunoprecipitation

Whole lysates (40 mg) were resolved by 8–12% sodium dodecyl sulfate-polyacrylamide gel electrophoresis. The proteins were then transferred to polyvinylidene difluoride membranes. The membranes were immunoblotted overnight at 4°C with primary antibodies against Sumo1, UBC9, Senp1 (c-12) (1:1000; Santa Cruz Biotechnology, Inc., CA, USA), Senp2, Serca2a (1:1000; Abcam, Cambridge, UK), and β-actin (1:5000; Beijing Zhongshan Golden bridge Biotechnology Co., Beijing, China). The corresponding secondary antibodies (1:5000; Beijing Zhongshan Golden bridge Biotechnology Co.) were then used for immunoblotting for 1 h. The enhanced chemiluminescence (ECL) working solution was then added dropwise to the membrane. Serca2a SUMOylation was detected by co-immunoprecipitation *in vivo*. Extracted protein (500 μg) samples were incubated with 2 μg of Sumo1 primary antibody or normal rabbit IgG (Cell Signaling Technology, Boston, UK) on a rotator at 4°C overnight. The protein sample was then eluted by the addition of 70 μL of the elution buffer and analyzed by Western blotting.[36] The target band was calculated using Image J software (ImageJ 1.47e, National Institutes of Health, Bethesda, MD, USA).

Immunofluorescence assay

Cardiomyocytes were fixed in 4% paraformaldehyde for 10 min and then permeabilized with 0.2% Triton X-100 for 10 min. The blocking buffer was then added for 30 min. The primary antibody (Senp1[c-12], Senp2, and Serca2a [1:200; Abcam]) was added after being washed to incubate the cells at 4°C overnight. The fluorescently labeled secondary antibody (goat anti-rabbit IgG H&L Alexa Fluor® 488 pre-adsorbed, goat anti-rabbit IgG H&L Alexa Fluor® 568 pre-adsorbed, and goat anti-mouse IgG H&L Alexa Fluor® 647 pre-adsorbed [1:100; Abcam]) was added to incubate the cells in the dark for 1 h. 4′,6-Diamidino-2′-phenylindole (DAPI) was also added in the dark for 10–30 min. Images were collected under a confocal microscope (Leica STELLARIS 5, Weztlar, Germany).[37]

Optimal multiplicity of infection (MOI) detection of each adenovirus

HL-1 cells were inoculated into 96-well plates at a density of 1×10^4/mL. HL-1 cells were divided into the following groups: Adenovirus (Ad)-GFP, Ad-RFP, Ad-Senp1, Ad-Senp1-shRNA1, Ad-Senp1-shRNA2, Ad-Senp1-shRNA3, Ad-Senp2, Ad-Senp2-shRNA1, Ad-Senp2-shRNA2, and Ad-Senp2-shRNA3. MOIs of 0, 10, 100, 300, and 500 were tested ($n = 3$). The Claycomb medium (Sigma-Aldrich, MO, USA) was replaced 6 h later. The ratio of GFP *vs*. RFP fluorescence-positive cells was determined by microscope 48 h later.

Triphenyltetrazolium chloride (TTC)-Evans blue staining

Mice were anesthetized 6 h after reperfusion. *In situ* ligation was again performed for the LAD artery. Then, 1% Evans blue (Sigma-Aldrich) was injected through the aortic end. The cardiac tissues were washed with 10% potassium chloride and preserved at −20°C for 30 min. The samples were then cut into five 1-mm-thick slices below the ligation line,each slice was at the same cross section. Then the slices were placed into 1% TTC (Sigma-Aldrich) solution at 37°C. The images were analyzed using Image J software. The blue area was the area not at risk (ANAR), while the red and white areas were the areas at risk (AAR), TTC and Evans blue-unstained areas were defined as infarcted area ($n = 3$).

Mice echocardiography

The I/RI procedure was performed in 28 C57BL/6J mice 3 days after viral injection. Twenty-four mice survived and were evaluated 6 h after I/RI ($n = 3$). A Vevo® 1100 Imaging System (FUJIFILM Visualsonics, Inc., Toronto, Canada) was used to record the left ventricular ejection fraction (LVEF) and left ventricular fractional shortening (LVFS). Each indicator was measured over three consecutive cardiac cycles and the average was used for analysis.

Statistical analysis

Statistical analysis was performed using GraphPad Prism 5 software (version 5, Windows version, GraphPad Software, San Diego, USA). Data were expressed as the mean ± standard error of mean (SEM). $\alpha = 0.05$. Intergroup comparisons were carried out using *t*-tests, while statistical comparisons among multiple groups were performed using ANOVA (one-way analysis of variance). Statistical significance was set two-tailed $P < 0.050$.

Results

Calcium-regulating effect of Serca2a in I/RI

We established mouse I/RI model, and cardiomyocytes were isolated using the Langendorff system (Thermo-Fisher) [Figure 1A]. Compared to the WT group, Serca2a mRNA was down-regulated in the I/RI group ($P < 0.001$), which was consistent with the Serca2a protein level trend in Figure 1B ($P < 0.010$). Serca2a mRNA expression in the *Serca2a* KO group decreased to 11.41 ± 9.55% ($P < 0.001$) of the WT group, while Serca2a protein expression decreased to 5.60 ± 1.38% ($P < 0.001$) of the WT group [Figure 1C]. Calcium transient detection results showed that when cardiomyocytes were stimulated at 0.5 Hz, the ΔFFI decreased in the I/RI (0.18 ± 0.09, $P < 0.010$) and *Serca2a* KO + I/RI (0.06 ± 0.13, $P < 0.010$) groups compared to the WT group (0.34 ± 0.17) [Figure 1D]. There was a reduction of ΔFFI in the *Serca2a* KO + I/RI group (0.06 ± 0.13) compared to the *Serca2a* KO (0.27 ± 0.11, $P < 0.001$) or I/RI groups (0.18 ± 0.09, $P < 0.010$). The contractility of a single cardiomyocyte was also determined. Compared to the WT group (4.13 ± 0.61 μm), the reduction was significant in the I/RI (1.71 ± 0.26 μm, $P < 0.010$) and *Serca2a* KO + I/RI (0.61 ± 0.21 μm, $P < 0.001$) groups. The reduction was also observed in the *Serca2a* KO + I/RI group compared to the *Serca2a* KO (4.21 ± 0.49 μm, $P < 0.001$) and I/RI (1.71 ± 0.26 μm, $P < 0.050$) groups. According to the above results, I/RI caused a down-regulation of Serca2a mRNA and protein levels. Following I/RI, the *Serca2a* KO group had a further reduction in the ΔFFI and contractility of a single cardiomyocyte.

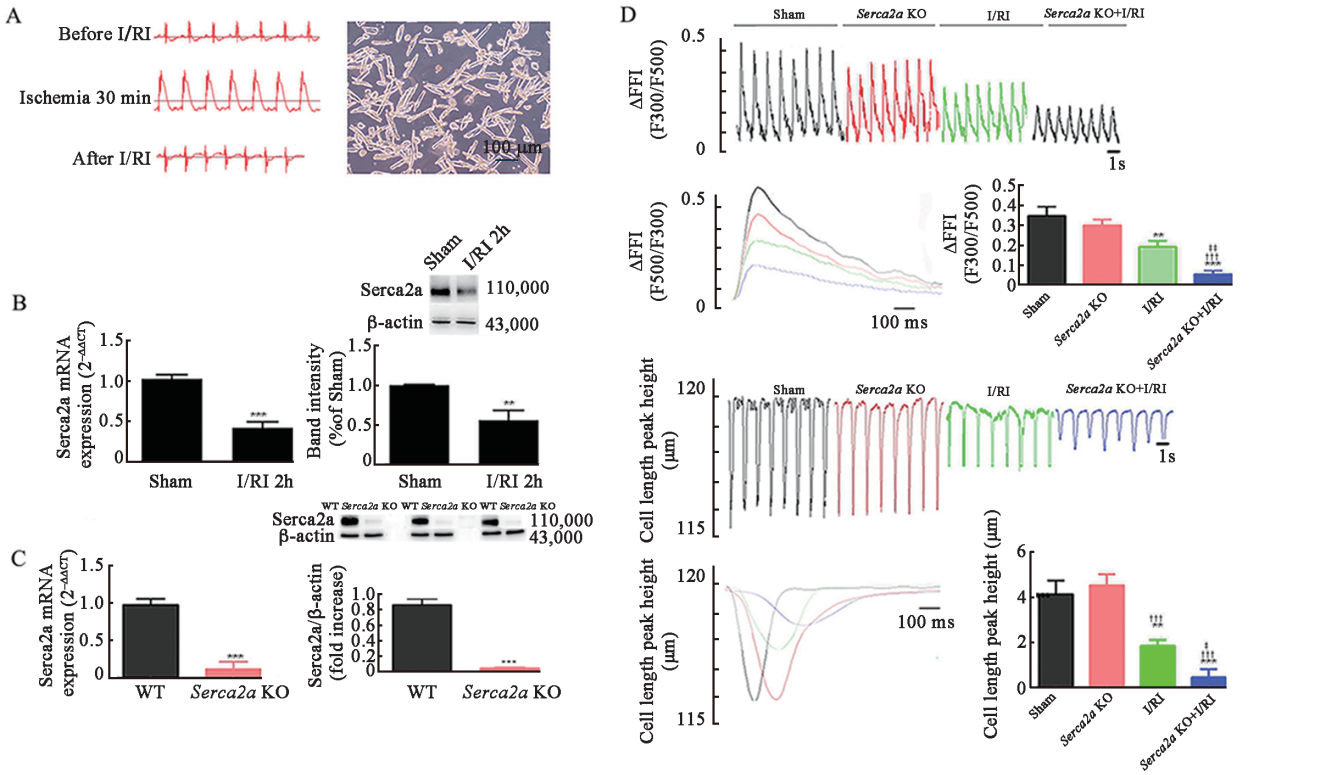

Figure 1: Calcium-regulating effect of SERCA2a in I/RI. (A) Construction of I/RI model in *Serca2a* KO mice, dynamic changes of electrocardiogram at different stages of myocardial I/RI, and isolation of cardiomyocytes using the Langendorff system (Scale bar=100 μm). (B) Serca2a mRNA and protein expression detected by RT-qPCR and Western blotting in C57BL/6J mice. (C) *Serca2a* KO efficiency detected by RT-qPCR and Western blotting at 2 weeks. (D) ΔFFI and contractility of a single cardiomyocyte under electrical stimulation. ΔFFI: changes of Fura-2 fluorescence intensity; I/RI: Ischemia/reperfusion injury; KO: Knockout; mRNA: messenger ribose nucleic acid; RT-qPCR: Quantitative real-time polymerase chain reaction; Serca2a: Sarcoplasmic reticulum calcium ATPase 2a; WT: Wild type. *Indicates comparison with the sham group, $^{*}P < 0.050$, $^{**}P < 0.010$, and $^{***}P < 0.001$. †Indicates comparison with the *Serca2a* KO group, $^{\dagger}P < 0.050$, $^{\dagger\dagger}P < 0.010$, and $^{\dagger\dagger\dagger}P < 0.001$. ‡Indicates comparison with the I/RI group, $^{\ddagger}P < 0.050$, $^{\ddagger\ddagger}P < 0.010$, and $^{\ddagger\ddagger\ddagger}P < 0.001$.

Changes in the expression and localization of SUMO-relevant proteins caused by I/RI

Expression of Sumo1 mRNA, protein, and relevant enzymes detected in C57BL/6J mice after I/RI

We established mice cardiac I/RI models *in vivo*. Expression levels of Sumo1, Ubc9, Senp1, and Senp2 mRNA and proteins were detected in C57BL/6J mice myocardium 0 h, 2 h, 6 h, 12 h, and 3 days after I/RI. Compared to the sham groups, Sumo1 mRNA level decreased between 12 h and 3 days after I/RI based on the RT-qPCR results [Figure 2A]. Senp1 and Senp2 mRNA expression levels peaked at 6 h after I/RI and decreased between 12 h and 3 days after I/RI. The same trend was observed in the expression of Sumo1, Senp1, and Senp2 proteins [Figure 2B]. There was no significant difference in the expression of Ubc9 mRNA and proteins among the groups. Based on the above results, Sumo1 mRNA and protein expression levels decreased after I/RI, while Senp1 and Senp2 mRNA and protein expression levels first increased and then decreased.

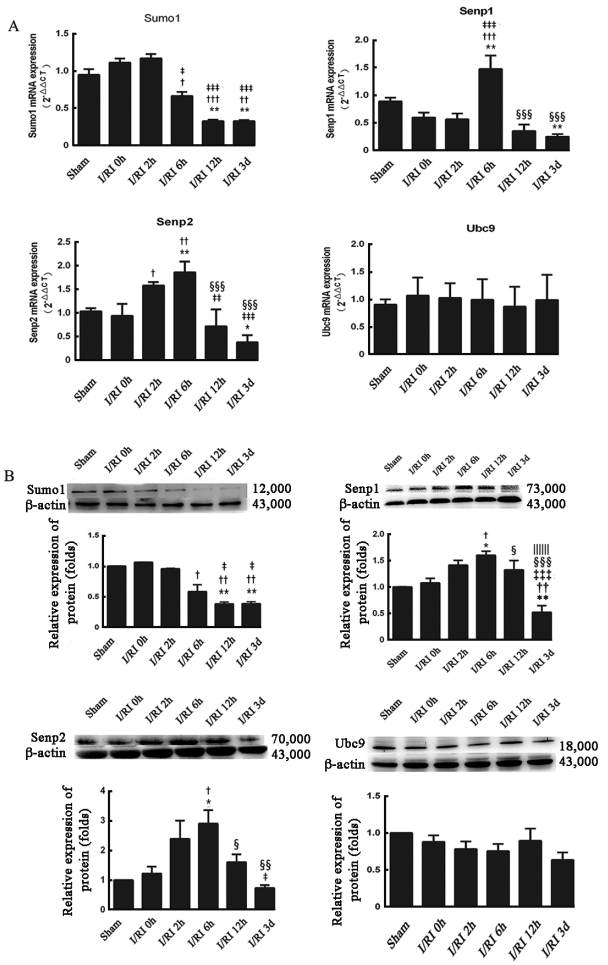

Figure 2: Detection of Sumo1, Ubc9, Senp1, and Senp2 mRNA and proteins in C57BL/6J mice at time of 0 h, 2 h, 6 h, 12 h, and 3 days after I/RI ($n = 3$). (A) RT-qPCR detection of Sumo1, Ubc9, Senp1, and Senp2 mRNA at different time points. (B) Western blotting detection of Sumo1, Ubc9, Senp1, and Senp2 proteins at different time points. I/RI: Ischemia/reperfusion injury; mRNA: messenger RNA; RT-qPCR: Quantitative real-time polymerase chain reaction; Senp1/2: sentrin/small ubiquitin-related modifier (SUMO) -specific protease 1/2; Ubc9: Ubiquitin-conjugating enzyme 9. *Indicates comparison with the sham group, $^{*}P$ <0.050, $^{**}P$ <0.010, and $^{***}P$ <0.001. †Indicates comparison with the I/RI 0 h group, $^{\dagger}P$ <0.050, $^{\dagger\dagger}P$ <0.010, and $^{\dagger\dagger\dagger}P$ <0.001. ‡Indicates comparison with the I/RI 2 h group, $^{\ddagger}P$ <0.050, $^{\ddagger\ddagger}P$ <0.010, and $^{\ddagger\ddagger\ddagger}P$ <0.001. §Indicates comparison with the I/RI 6 h group, $^{\S}P$ <0.050, $^{\S\S}P$ <0.010, and $^{\S\S\S}P$ <0.001. $^{\|}$Indicates comparison with the I/RI 12 h group, $^{\|}P$ <0.050, $^{\|\|}P$ <0.010, and $^{\|\|\|}P$ <0.001.

Expression of SUMO protein and relevant enzymes in mouse cardiomyocytes and HL-1 cells after sI/RI

Expression levels of Sumo1, Ubc9, Senp1, and Senp2 mRNA and proteins were determined 0 h, 2 h, 6 h, 12 h, and 3 days after sI/RI. The cardiomyocytes were isolated using the Langendorff system (ThermoFisher). They were rod-like and had a regular arrangement of clear edges and Z-lines [Figure 3A, left panel]. The right panel in Figure 3A showed a reduction in the percentage of rod-shaped cardiomyocytes, obscure Z-lines on the edges, and some rounded cells 6 h after sI/RI. Compared to the sham group, expression of Sumo1 mRNA decreased between 12 h and 3 days after sI/RI [Figure 3B]. The expression of Senp1 and Senp2 mRNA peaked at 6 h and decreased between 12 h and 3 days after sI/RI. There was no significant difference in Ubc9 mRNA among the groups. The Western blot results showed the same trend as the mRNA [Figure 3C].

The influence of sI/RI on the expression of Sumo1, Ubc9, Senp1, and Senp2 mRNA and proteins was assessed in HL-1 cells. sI/RI was induced with an ischemic duration of 1.5 h and reperfusion duration of 0 h, 2 h, 6 h, 12 h, and 3 days. HL-1 cells were long and spindle-shaped with good adherence [Figure 3D]. The cell bodies were thinned and some cells became rounded 6 h after sI/RI. Compared to the control group, the expression of Sumo1, Senp1, and Senp2 mRNA peaked at 12 h after sI/RI and declined at the 3-day time point [Figure 3E]. There was no significant difference in the expression of Ubc9 mRNA among the groups. The Western blot results showed the same trend as the mRNA [Figure 3F].

Changes in localization of Serca2a, Senp1, and Senp2 caused by sI/RI

Protein distribution was observed under a laser confocal microscope. The cardiomyocytes isolated from normal mice have regularly stripes, which were the Z-lines [Figure 4]. The nuclei were stained by DAPI. Serca2a protein was detected in the cytoplasm and nuclei, binded by Alexa Fluor® 568 with orange fluorescence and accumulating at the Z-lines. Senp1 protein was also detected in the cytoplasm and nuclei, binded by Alexa Fluor® 647 with red fluorescence and accumulating at the Z-lines. Senp2 protein was detected in the cytoplasm and nuclei, binded by Alexa Fluor® 488 with green fluorescence. Co-localization of Senp1 and Serca2a, but not of Senp2 and Serca2a, was observed at the Z-lines [Figure 4].

The localization of Senp1, Senp2, and Serca2a in cardiomyocytes was observed to assess the influence of sI/RI on these proteins in HL-1. Senp1 and Serca2a were detected

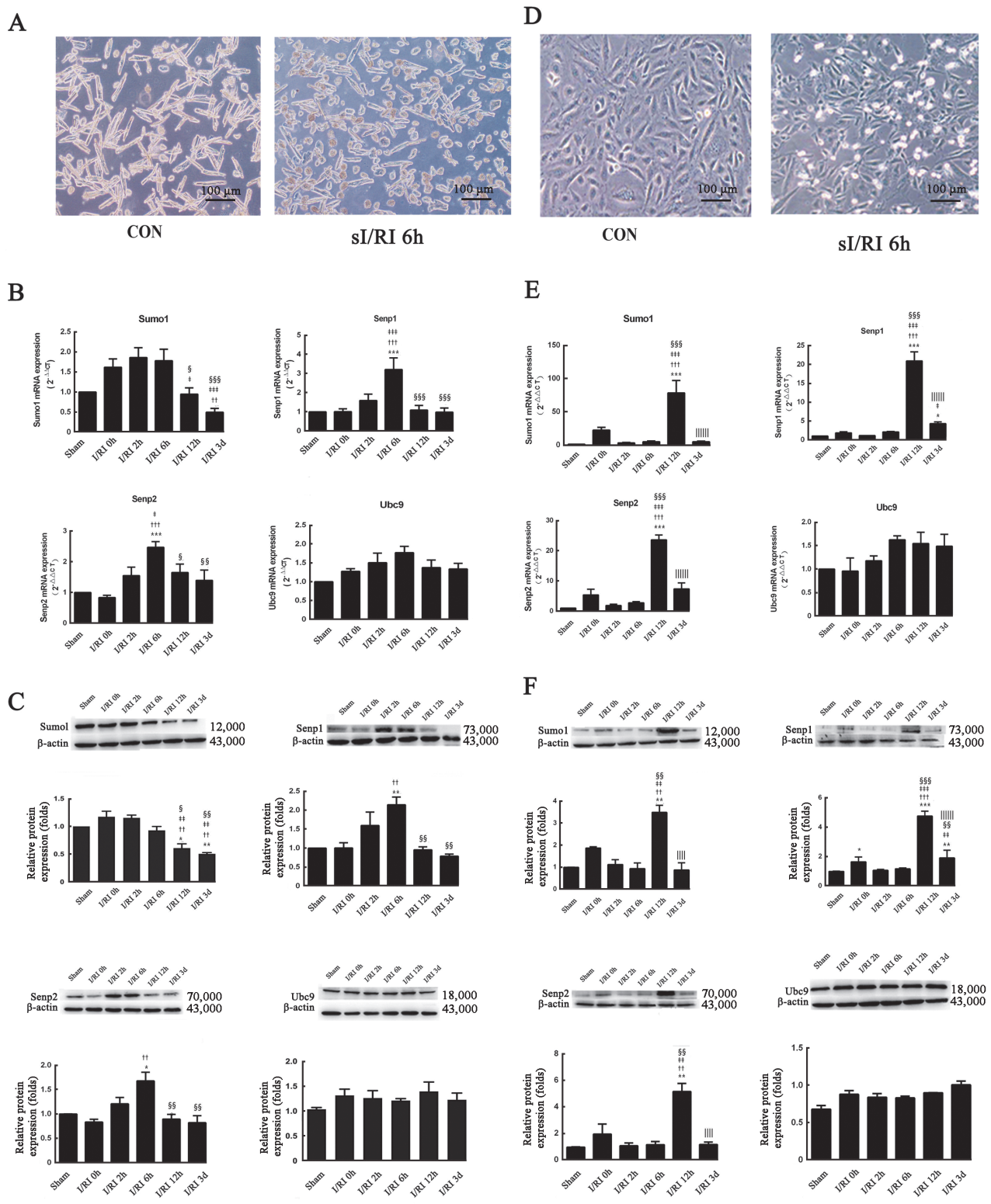

Figure 3: Expression of Sumo1, Ubc9, Senp1, and Senp2 mRNA and proteins in cardiomyocytes and HL-1 cells at time 0 h, 2 h, 6 h, 12 h, and 3 days after sI/RI ($n = 3$). (A) Morphology of cardiomyocytes isolated from C57BL/6J mice before and after I/RI (Scale bar=100 μm). (B) RT-qPCR detection of Sumo1, Ubc9, Senp1, and Senp2 mRNA in cardiomyocytes. (C) Western blot detection of Sumo1, Ubc9, Senp1, and Senp2 proteins in cardiomyocytes. (D) Morphology of HL-1 (Scale bar=100 μm). (E) RT-qPCR detection of Sumo1, Ubc9, Senp1, and Senp2 mRNA in HL-1 cells. (F) Western blot detection of Sumo1, Ubc9, Senp1, and Senp2 proteins in HL-1 cells. CON: Control; I/RI: Ischemia/reperfusion injury; RT-qPCR: Quantitative real-time polymerase chain reaction; Senp1/2: sentrin/small ubiquitin-related modifier (SUMO)-specific protease 1/2; sI/RI: simulation I/RI; Ubc9:Ubiquitin-conjugating enzyme 9. *Indicates comparison with the sham group, $^{*}P < 0.050$, $^{**}P < 0.010$, and $^{***}P < 0.001$. †Indicates comparison with the I/RI 0 h group, $^{\dagger}P < 0.050$, $^{\dagger\dagger}P < 0.010$, and $^{\dagger\dagger\dagger}P < 0.001$. ‡Indicates comparison with the I/RI 2 h group, $^{\ddagger}P < 0.050$, $^{\ddagger\ddagger}P < 0.010$, and $^{\ddagger\ddagger\ddagger}P < 0.001$. §Indicates comparison with the I/RI 6 h group, $^{\S}P < 0.050$, $^{\S\S}P < 0.010$, and $^{\S\S\S}P < 0.001$. $^{\|}$Indicates comparison with the I/RI 12 h group, $^{\|}P < 0.050$, $^{\|\|}P < 0.010$, and $^{\|\|\|}P < 0.001$.

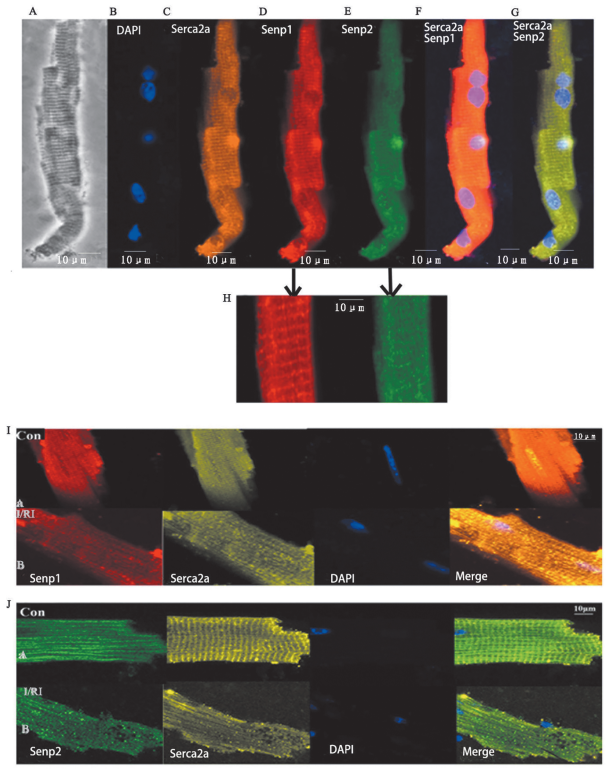

Figure 4: Localization of Senp1, Senp2, and Serca2a in cardiomyocytes using immunofluorescence and influence of I/RI on localization (Scale bar=10 μm; $n = 3$). (A) Bright-field image of cardiomyocytes. (B) DAPI staining of cardiomyocytes (blue). (C) Serca2a protein staining with Alexa Fluor® 568 (orange). (D) Senp1 protein staining with Alexa Fluor® 647 (red). (E) Senp2 protein staining with Alexa Fluor® 488 (green). (F) Co-localization of Senp1 and Serca2a. (G) Co-localization of Senp2 and Serca2a. (H) Magnification of Senp1 and Senp2 location. (I) Localization of Serca2a and Senp1 proteins in cardiomyocytes 6 h after I/RI. (J) Localization of Serca2a and Senp2 proteins in cardiomyocytes 6 h after I/RI. Con: Control; DAPI: 4′,6-Diamidino-2′-phenylindole; I/RI: Ischemia/reperfusion injury; Senp1/2: sentrin/small ubiquitin-related modifier (SUMO)-specific protease 1/2; Ubc9:Ubiquitin-conjugating enzyme 9.

in the cytoplasm and nuclei in the control group. Senp1 showed no significant change 6 h after sI/RI [Figure 4I]. Similar detection of Senp2 and Serca2a showed that the cytoplasmic expression of Senp2 was locally enhanced 6 h after sI/RI [Figure 4J]. These results indicated a local accumulation of Senp2 in the cytoplasm after sI/RI.

Mechanism of Senp mediated Serca2a de-SUMOylation to exacerbate myocardial I/RI

Efficiency of adenoviral transfection of Senp1 and Senp2 in HL-1 cells

The viral titer was 1×10^{11}. The cells were infected with MOI values of 0, 10, 100, 300, and 500 for 48 h. The percentages of GFP- and RFP-positive cells at MOI = 500 were 94.33 ± 1.52% and 91.66 ± 2.51% in the Ad-GFP and Ad-RFP groups, respectively. A few cells became rounded at MOI = 300 in the Ad-Senp1 (infecting efficiency 81.33 ± 1.52%) and Ad-Senp2 (infecting efficiency 83.66 ± 1.52%) groups but most of the cells became rounded and their status deteriorated at MOI = 500. The percentage of GFP-positive cells at MOI = 500 was 88.67 ± 3.21%, 87.33 ± 2.52%, and 93.67 ± 3.21% in the Ad-Senp1-shRNA1, Ad-Senp1-shRNA2, and Ad-Senp1-shRNA3 groups, respectively. The percentage of RFP-positive cells in these groups was 94.67 ± 0.58%, 94.66 ± 2.08%, and 93.67 ± 3.21%, respectively. Therefore, for the Ad-GFP, Ad-RFP, Ad-Senp1-shRNA, and Ad-Senp2-shRNA groups, the optimal MOI was 500. For the Ad-Senp1 and Ad-Senp2 groups, the optimal MOI was 300. In addition, overexpression of Senp1 and Senp2 caused the cell shape changing from spindle to round in morphology and the cells could not attach and grow properly [Supplementary Figures 1A and B, http://links.lww.com/CM9/B612].

Western blotting was used to detect Senp1 and Senp2 protein expression 48 h after viral infection of HL-1 cells and 3 days after intramyocardial injection of the viral vector. There was no significant difference in Senp1 and Senp2 expression in the Ad-GFP and Ad-RFP groups compared to the control group, but there was a significant up-regulation of Senp1 in the Ad-Senp1 group and Senp2 in the Ad-Senp2 group [Supplementary Figure 1C, http://links.lww.com/CM9/B612]. Compared to the control group, the down-regulation of Senp1 and Senp2 was greatest in the Ad-Senp1-shRNA3 and Ad-Senp2-shRNA3 groups.

The *in vivo* detection results are shown in Supplementary Figure 1C, http://links.lww.com/CM9/B612. The Ad-GFP and Ad-RFP groups did not show significant differences in Senp1 and Senp2 protein expression compared to the sham group, while the Ad-Senp1 group had a dramatic increase in Senp1, and Senp2 was increased in the Ad-Senp2 group. The expression of Senp1 and Senp2 demonstrated the greatest decrease in the Ad-Senp1-shRNA3 and Ad-Senp2-shRNA3 groups compared to the sham group, respectively.

Co-immunoprecipitation to detect Serca2a SUMOylation *in vivo* with overexpression/inhibition of Senp1 and Senp2

The chest was opened in C57BL/6J mice to perform intramyocardial injection of the adenoviral vectors. The I/RI models were generated 3 days later and cardiac tissues were harvested 6 h after I/RI. Protein samples were then extracted for co-immunoprecipitation experiments [Figure 5A]. Serca2a SUMOylation decreased in the I/RI, Ad-RFP + I/RI, and Ad-GFP + I/RI groups compared to the sham group. Compared to the I/RI, Ad-GFP + I/RI, and Ad-RFP + I/RI groups, Serca2a SUMOylation decreased in the Ad-Senp1 + I/RI group, while no increase was observed in the Ad-Senp1-shRNA3 + I/RI group [Figure 5B]. Serca2a SUMOylation further decreased in the Ad-Senp2 + I/RI group compared to the I/RI, Ad-GFP + I/RI, and Ad-RFP + I/RI groups, while Serca2a SUMOylation increased in the Ad-Senp2-shRNA3 + I/RI group. The above results indicated that I/RI caused a reduction in Serca2a SUMOylation, while an overexpression of Senp1 and Senp2 decreased Serca2a SUMOylation in the cardiomyocytes. Serca2a SUMOylation was restored by inhibiting Senp2 expression, while infection with Ad-Senp1-shRNA3 did not reverse the reduction in Serca2a SUMOylation caused by I/RI.

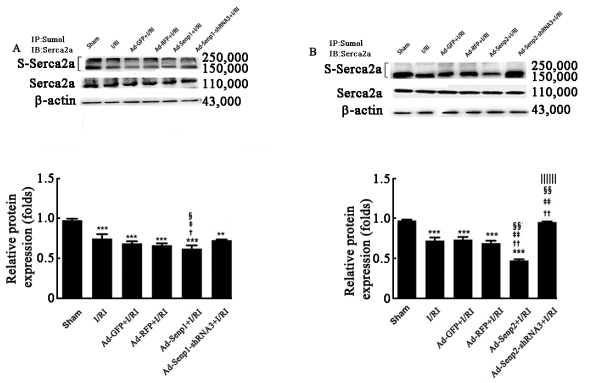

Figure 5: Co-immunoprecipitation to detect Serca2a SUMOylation *in vivo* with overexpression/inhibition of Senp1 and Senp2 ($n = 3$). (A) Serca2a SUMOylation *in vivo* with overexpression/inhibition of Senp1. (B) Serca2a SUMOylation *in vivo* with overexpression/inhibition of Senp2. Ad: Adenovirus; GFP: Green florescent protein; IB: Immunoblotting; IP: Immunoprecipitation; I/RI: Ischemia/reperfusion injury; RFP: Red florescent protein; Senp1/2: sentrin/small ubiquitin-related modifier (SUMO) -specific protease 1/2; Serca2a: Sarcoplasmic reticulum calcium ATPase 2a; S-Serca2a: SUMOylated Serca2a. *Indicates comparison with the sham group, $^{*}P$ <0.050, $^{**}P$ <0.010, and $^{***}P$ <0.001. †Indicates comparison with the I/RI group, $^{\dagger}P$ <0.050, $^{\dagger\dagger}P$ <0.010, and $^{\dagger\dagger\dagger}P$ <0.001. ‡Indicates comparison with the Ad-GFP + I/RI group, $^{\ddagger}P$ <0.050, $^{\ddagger\ddagger}P$ <0.010, and $^{\ddagger\ddagger\ddagger}P$ <0.001. §Indicates comparison with the Ad-RFP + I/RI group, $^{\S}P$ <0.050, $^{\S\S}P$ <0.010, and $^{\S\S\S}P$ <0.001. $^{\|}$Indicates comparison with Ad-Senp1 + I/RI or Ad-Senp2 + I/RI group, $^{\|}P$ <0.050, $^{\|\|}P$ <0.010,

Detection of Senp1 and Senp2 influence on the infarct area and cardiac function *in vivo*

Intramyocardial injection of Senp1 and Senp2 adenoviruses was performed. The I/RI models were generated 3 days later, and TTC-Evans blue staining was performed 6 h after I/RI. There was an increase in the percentage of infarct area in the I/RI, Ad-GFP + I/RI, and Ad-RFP + I/RI groups (37.90 ± 2.05%, 37.81 ± 1.50%, and 38.13 ± 2.22%, respectively, P <0.001) compared to the sham group [Figure 6]. The percentage of AAR was higher in the Ad-Senp1 + I/RI and Ad-Senp2 + I/RI groups (62.88 ± 1.81% and 71.34 ± 2.55%, respectively, P <0.001) than the I/RI, Ad-GFP + I/RI, and Ad-RFP + I/RI groups. There was no reduction in the percentage of AAR in the Ad-Senp1-shRNA3 + I/RI group (54.61 ± 1.42%, P <0.001), while the percentage decreased to 20.85 ± 2.65% in the Ad-Senp2-shRNA3 + I/RI group (P <0.001).

The ultrasonic examination results are shown in Figure 7. The ejection fractions (EFs) of the I/RI, Ad-GFP + I/RI, and Ad-RFP + I/RI groups were lower than those of the sham group (39.96 ± 6.70%, P <0.001; 50.02 ± 4.70%, P <0.050; and 46.35 ± 4.67%, P <0.010 *vs.* 66.35 ± 1.73%). The EFs of the Ad-Senp1 + I/RI and Ad-Senp1-shRNA3 + I/RI groups were 53.40 ± 3.36% (P >0.050) and 54.18 ± 1.01% (P >0.050), respectively, with no significant difference compared to the I/RI, Ad-GFP + I/RI, and Ad-RFP + I/RI groups (P >0.050). The EF of the Ad-Senp2 + I/RI groups further decreased to 28.96 ± 2.22% (P <0.050). The EF of the Ad-Senp2-shRNA3 + I/RI group was restored compared to the Ad-Senp2 + I/RI group (60.19 ± 7.15%, P <0.010). The fractional shortening (FS) values of the I/RI, Ad-GFP + I/RI, and Ad-RFP + I/RI groups compared to 35.92 ± 1.36% in the sham group were 19.16 ± 3.54% (P <0.001), 25.13 ± 3.08% (P <0.050), and 22.88 ± 2.60% (P <0.010), respectively. The FS of the Ad-Senp1 + I/RI and Ad-Senp1-shRNA3 + I/RI groups were 27.03 ± 2.25% (P >0.050) and 27.36 ± 0.74% (P >0.050), respectively and showed no statistically significant difference compared to the I/RI, Ad-GFP + I/RI, and Ad-RFP + I/RI groups, while the FS of the Ad-Senp2 + I/RI group decreased to 13.14 ± 1.14% (P <0.050). The FS of the Ad-Senp2-shRNA3 + I/RI group was restored to 31.38 ± 4.80% (P <0.010), indicating a significant difference from the Ad-Senp2 + I/RI group.

Discussion

With the advances in reperfusion techniques, the incidence of I/RI has been rising at an alarming rate. The severity of I/RI is closely associated with the duration of myocardial ischemia, distribution of coronary microcirculation, oxygen supply/demand imbalance, and reperfusion regulation.[38] The molecular mechanism underlying I/RI needs to be elucidated to develop effective treatments to protect the myocardium and improve the long-term prognosis following I/RI.[39–42]

Regulatory role of SERCA2a in calcium homeostasis after I/RI

Regulating the important steps in the mechanism underlying calcium overload, such as antagonizing mitochondrial calcium ion channels and Na^+–Ca^{2+} or Na^+–H^+ exchangers, can significantly reduce the intracellular calcium ion concentration and infarct size.[8] Therefore, we attempted to identify the regulatory targets of calcium overload in I/RI to attenuate calcium overload.

A decline in SERCA2a function and vitality is a shared feature in heart failure patients or animal models of heart failure.[43,44] Restoring SERCA2a expression and function through transgenic therapy or medication can help improve systolic and diastolic functions.[17,45] Recently, Jiang *et al*[46] have demonstrated that overexpression of SERCA2a protected myocardium from I/RI and recovered postischemic function via anti-necrotic, anti-apoptotic, and pro-autophagy signaling pathways. However, no study has been conducted on *Serca2a* KO mice to achieve loss of function of *Serca2a* to verify the role in maintaining calcium homeostasis following I/RI. The present study utilized *Serca2a* KO mice to demonstrate *Serca2a* regulative role in calcium homeostasis in I/RI. The experimental results showed that I/RI downregulated the myocardial *Serca2a* expression, which caused a decrease in calcium transient and contractility of a single cardiomyocyte. These indices in *Serca2a* KO + I/RI groups decreased significantly compared to those in the *Serca2a* KO or I/RI groups. The above results indicated that SERCA2a maintained calcium homeostasis in cardiomyocytes and could reduce Ca^{2+} overload in the cytoplasm after I/RI.

Changes of SUMO1 protein and SUMOylation/deSUMOylation enzymes after I/RI

SUMOylation and deSUMOylation are indispensable to the cardiac physiology. Few studies have been conducted

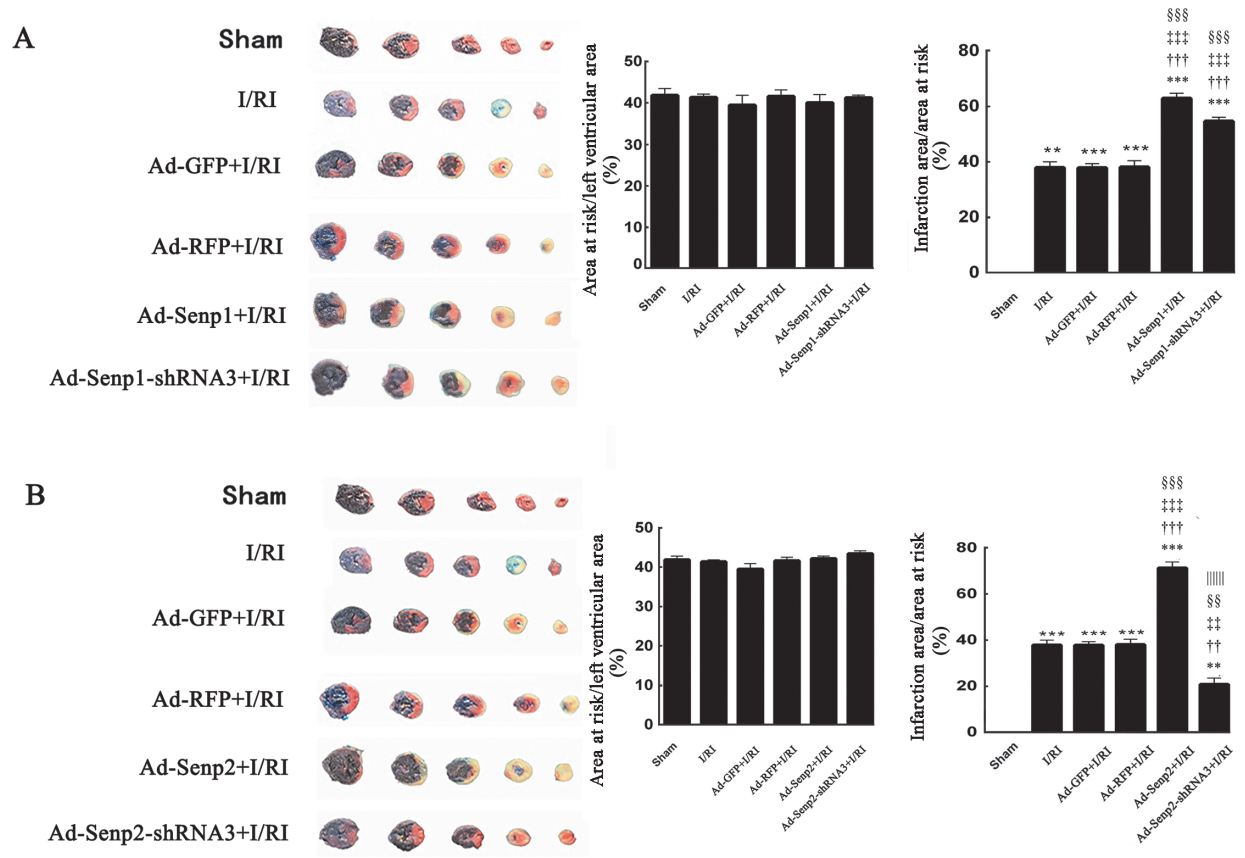

Figure 6: Infarct size based on TTC-Evans blue staining in mice with overexpression or inhibition of Senp1 and Senp2 following I/RI ($n = 3$). (A) Infarct size detected by TTC-Evans blue staining with Senp1 targeting intervention after I/RI. (B) Infarct size detected by TTC-Evans blue staining with Senp2 targeting intervention after I/RI. The blue area was the area not at risk, the red and white areas were the AAR, white area was also infarction area; AAR: Areas at risk; Ad: Adenovirus; GFP: Green florescent protein; I/RI: Ischemia/reperfusion injury; RFP: Red florescent protein; Senp1/2: sentrin/small ubiquitin-related modifier (SUMO)-specific protease 1/2; TTC: triphenyltetrazolium chloride. *Indicates comparison with the sham group, $^{*}P$ <0.050, $^{**}P$ <0.010, and $^{***}P$ <0.001. †Indicates comparison with the I/RI group, $^{\dagger}P$ <0.050, $^{\dagger\dagger}P$ <0.010, and $^{\dagger\dagger\dagger}P$ <0.001. ‡Indicates comparison with the Ad-GFP + I/RI group, $^{\ddagger}P$ <0.050, $^{\ddagger\ddagger}P$ <0.010, and $^{\ddagger\ddagger\ddagger}P$ <0.001. §Indicates comparison with the Ad-RFP + I/RI group, $^{\S}P$ <0.050, $^{\S\S}P$ <0.010, and $^{\S\S\S}P$ <0.001. $^{\|}$Indicates comparison with Ad-Senp1 + I/RI or Ad-Senp2 + I/RI group, $^{\|}P$ <0.050, $^{\|\|}P$ <0.010, and $^{\|\|\|}P$ <0.001.

involving the role of the SUMO system in I/RI. Comerford *et al*[47] have reported an overall increase in the SUMO-modified protein level after *in vitro* hypoxic culture. SUMOylation regulated the stability of hypoxia-inducible factor (HIF)-1α,[48,49] thereby regulating the glycolytic pathway.[50] The alteration in SENPs may be closely related to cardiac disorders. For example, the lack of the *Senp2* gene caused cardiac hypoplasia in mice, whereas its overexpression was associated with cardiomyopathy and congenital heart defects.[30]

Among the studies on the nervous system, Cimarosti *et al*[51] have reported up-regulation of SENP1 in oxygen and glucose deprivation (OGD) in hippocampal neurons. Overexpression of SENP1 resulted in lower SUMOylation and higher susceptibility of the cells to death. Using the I/RI model of the middle cerebral artery, Zhang *et al*[52] have reported that apoptosis was increased in *Senp1* KO mice. Cheng *et al*[53] have proposed that hypoxia-induced SUMOylation of HIF-1α was a dynamic process in the cardiovascular system. Gu *et al*[32] have suggested that SENP1 protected against myocardial I/RI by regulating SUMOylation of HIF-1α. Xia *et al*[54] have proposed that inhibition of SENP6 restrained cerebral I/RI by regulating annexin-A1 nuclear translocation-associated neuronal apoptosis.

The present study observed the effect of sI/RI on the expression and localization of Sumo1, Senp1, and Senp2 in cardiomyocytes. Sumo1 expression decreased in cardiac tissues and cardiomyocytes following I/RI at the cellular level and *in vivo*. However, the situation was more complex in HL-1 cells, where Sumo1 expression level peak was detected 12 h after sI/RI, which then decreased 3 days after sI/RI. This difference indicated that hypoxia/reoxygenation might stimulate the expression of Sumo1 to adapt to environmental changes in HL-1 cells, although the specific mechanism remained unclear. Senp1 and Senp2 expression showed a consistent variation. In mouse cardiac tissues and cardiomyocytes, Senp1 and Senp2 expression first increased and then decreased. Combining this evidence with the immunofluorescence assay results, no local up-regulation of SENP1 after sI/RI was observed. In contrast, SENP2 expression increased locally in the cytoplasm after sI/RI. Indeed, lower SUMOylation of SERCA2a may be related to the up-regulation of SENP2 following sI/RI.

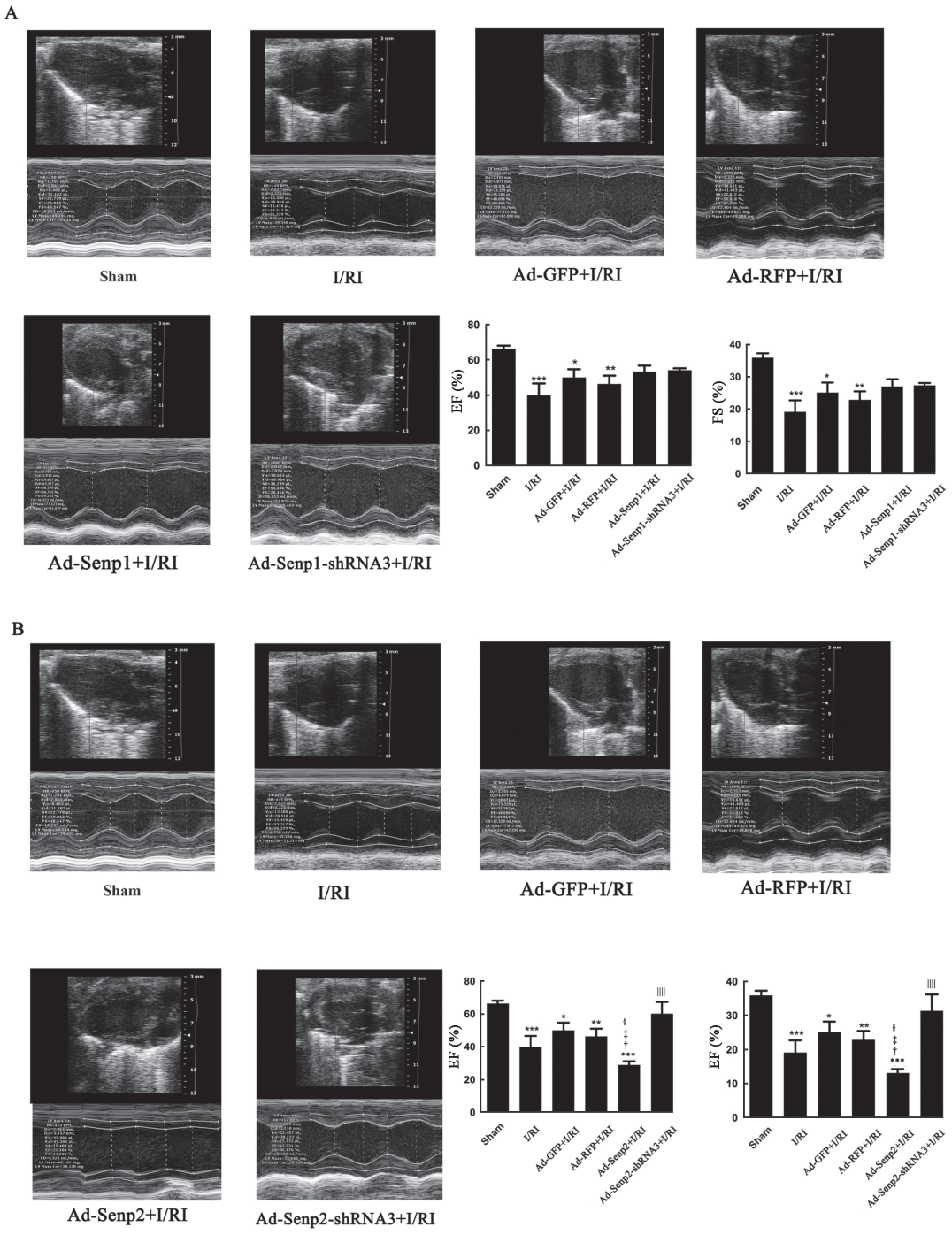

Figure 7: Cardiac function based on ultrasonic examination of mice with overexpression or inhibition of Senp1 and Senp2 following I/RI ($n = 3$). (A) Cardiac function detection in mice receiving Senp1-targeting intervention. (B) Cardiac function detection in mice receiving Senp2-targeting intervention. EF: Ejection fraction; FS: Fractional shortening; GFP: Green florescent protein; I/RI: Ischemia/reperfusion injury; RFP: Red florescent protein; Senp1/2: sentrin/small ubiquitin-related modifier (SUMO)-specific protease 1/2; shRNA: Short hairpin ribose nucleic acid. *Indicates comparison with the sham group, $^{*}P < 0.050$, $^{**}P < 0.010$, and $^{***}P < 0.001$. †Indicates comparison with the I/RI group, $^{\dagger}P < 0.050$, $^{\dagger\dagger}P < 0.010$, and $^{\dagger\dagger\dagger}P < 0.001$. ‡Indicates comparison with the Ad-GFP + I/RI group, $^{\ddagger}P < 0.050$, $^{\ddagger\ddagger}P < 0.010$, and $^{\ddagger\ddagger\ddagger}P < 0.001$. §Indicates comparison with the Ad-RFP + I/RI group, $^{\S}P < 0.050$, $^{\S\S}P < 0.010$, and $^{\S\S\S}P < 0.001$. ‖Indicates comparison with Ad-Senp1 + I/RI or Ad-Senp2 + I/RI group, $^{\|}P < 0.050$, $^{\|\|}P < 0.010$, and $^{\|\|\|}P < 0.001$.

I/RI activated SENP1 and SENP2 protein expression and promoted deSUMOylation of SERCA2a

SUMOylation is an important post-translational modification of SERCA2a. Kho *et al*[25] have suggested that only SUMO1 could bind to SERCA2a in cardiomyocytes, enhancing the stability of SERCA2a and restoring the function of the calcium pump. However, the reasons underlying the decreased SUMOylation of SERCA2a following I/RI have not been confirmed. We speculated that I/RI might activate deSUMOylation enzymes expression in the cells to accelerate the deSUMOylation

process, thus promote deSUMOylation of SERCA2a. To test this assumption, adenoviral vectors overexpressing or inhibiting Senp1 and Senp2 were constructed. The results of the co-immunoprecipitation assay showed that I/RI reduced SUMOylation of Serca2a. Overexpression of Senp1 and Senp2 decreased SUMOylation of Serca2a in cardiac tissues, indicating that I/RI-activated expression of Senp1 and Senp2 was one reason for the decrease in Serca2a SUMOylation. Infecting cells with the Ad-Senp2-shRNA3 vector restored SUMOylation of Serca2a, but infection with the Ad-Senp1-shRNA3 vector failed to restore it. Thus, SENP2 was the primary regulator of SUMOylation of SERCA2a after I/RI. To verify the relationship between SUMOylation of SERCA2a and heart function, infarct size and cardiac function were determined *in vivo*. The results indicated that overexpression of SENP1 and SENP2 aggravated the infarct size. Inhibiting SENP2, instead of SENP1, reduced the infarct size and cardiac function.

Limitations and summary

However, a limitation of the present study was that we did not explore calcium transient and diastolic/systolic function of cardiomyocytes with overexpression or inhibition of SENP1 and SENP2 by adenoviral vectors. The location and regulation mechanisms of SENP2 on SERCA2a deSUMOylation also need to be further investigated.

The present study explored the regulatory role of Serca2a in calcium homeostasis of cardiomyocytes following I/RI. *Serca2a* KO further aggravated the calcium overload, which was considered to be the mechanism underlying I/RI. Based on the changes in the expression and localization of Sumo1 and relevant enzymes, I/RI decreased the Sumo1 expression, upregulated Senp1 and Senp2 expression, and enhanced the cytoplasmic localization of Senp2. Serca2a deSUMOylation was promoted by inducing overexpression of Senp1 and Senp2 and restored only by inhibiting Senp2, which reduced the infarct size and restored cardiac function. Therefore, SENP2 was identified as a target for attenuating myocardial I/RI.

Funding

This work was supported by grants from the Natural Science Foundation of Jiangsu Province (No. BK20190988), the Scientific Research Project of Jiangsu Health Committee (No. H2018005), the Key Research and Development Program of Xuzhou (No. KC20097), and the Postgraduate Research & Practice Innovation Program of Jiangsu Province (No. KYCX21_2671).

Conflicts of interest

None.

References

1. Wilmot KA, O'Flaherty M, Capewell S, Ford ES, Vaccarino V. Coronary heart disease mortality declines in the United States from 1979 through 2011: Evidence for stagnation in young adults, especially women. Circulation 2015;132:997–1002. doi: 10.1161/CIRCULATIONAHA.115.015293.
2. Ndrepepa G, Colleran R, Kastrati A. Reperfusion injury in ST-segment elevation myocardial infarction: The final frontier. Coron Artery Dis 2017;28:253–262. doi: 10.1097/MCA.0000000000000468.
3. Davidson SM, Ferdinandy P, Andreadou I, Bøtker HE, Heusch G, Ibáñez B, *et al*. Multitarget strategies to reduce myocardial ischemia/reperfusion injury: JACC review topic of the week. J Am Coll Cardiol 2019;73:89–99. doi: 10.1016/j.jacc.2018.09.086.
4. Heusch G. Myocardial stunning and hibernation revisited. Nat Rev Cardiol 2021;18:522–536. doi: 10.1038/s41569-021-00506-7.
5. Hausenloy DJ, Yellon DM. Ischaemic conditioning and reperfusion injury. Nat Rev Cardiol 2016;13:193–209. doi: 10.1038/nrcardio.2016.5.
6. Chi HJ, Chen ML, Yang XC, Lin XM, Sun H, Zhao WS, *et al*. Progress in therapies for myocardial ischemia reperfusion injury. Curr Drug Targets 2017;18:1712–1721. doi: 10.2174/1389450117666160401120308.
7. Wang NF, Bai CX. Bone marrow-derived mesenchymal stem cells modulate autophagy in RAW264.7 macrophages via the phosphoinositide 3-kinase/protein kinase B/heme oxygenase-1 signaling pathway under oxygen-glucose deprivation/restoration conditions. Chin Med J 2021;134:699–707. doi: 10.1097/cm9.0000000000001133.
8. Wang R, Wang M, He S, Sun G, Sun X. Targeting calcium homeostasis in myocardial ischemia/reperfusion injury: An overview of regulatory mechanisms and therapeutic reagents. Front Pharmacol 2020;11:872. doi: 10.3389/fphar.2020.00872.
9. Vassalle M, Lin CI. Calcium overload and cardiac function. J Biomed Sci 2004;11:542–565. doi: 10.1007/bf02256119.
10. Korf-Klingebiel M, Reboll MR, Polten F, Weber N, Jäckle F, Wu X, *et al*. Myeloid-derived growth factor protects against pressure overload-induced heart failure by preserving sarco/endoplasmic reticulum Ca(2+)-ATPase expression in cardiomyocytes. Circulation 2021;144:1227–1240. doi: 10.1161/circulationaha.120.053365.
11. Zhihao L, Jingyu N, Lan L, Michael S, Rui G, Xiyun B, *et al*. SERCA2a: A key protein in the Ca^{2+} cycle of the heart failure. Heart Fail Rev 2020;25:523–535. doi: 10.1007/s10741-019-09873-3.
12. Kho C, Lee A, Hajjar RJ. Altered sarcoplasmic reticulum calcium cycling – Targets for heart failure therapy. Nat Rev Cardiol 2012;9:717–733. doi: 10.1038/nrcardio.2012.145.
13. Luraghi A, Ferrandi M, Barassi P, Arici M, Hsu SC, Torre E, *et al*. Highly selective SERCA2a activators: Preclinical development of a congeneric group of first-in-class drug leads against heart failure. J Med Chem 2022;65:7324–7333. doi: 10.1021/acs.jmedchem.2c00347.
14. Ding L, Su XX, Zhang WH, Xu YX, Pan XF. Gene expressions underlying mishandled calcium clearance and elevated generation of reactive oxygen species in the coronary artery smooth muscle cells of chronic heart failure rats. Chin Med J 2017;130:460–469. doi: 10.4103/0366-6999.199825.
15. Miyamoto MI, del Monte F, Schmidt U, DiSalvo TS, Kang ZB, Matsui T, *et al*. Adenoviral gene transfer of SERCA2a improves left-ventricular function in aortic-banded rats in transition to heart failure. Proc Natl Acad Sci U S A 2000;97:793–798. doi: 10.1073/pnas.97.2.793.
16. Zsebo K, Yaroshinsky A, Rudy JJ, Wagner K, Greenberg B, Jessup M, *et al*. Long-term effects of AAV1/SERCA2a gene transfer in patients with severe heart failure: Analysis of recurrent cardiovascular events and mortality. Circ Res 2014;114:101–108. doi: 10.1161/CIRCRESAHA.113.302421.
17. Samuel TJ, Rosenberry RP, Lee S, Pan Z. Correcting calcium dysregulation in chronic heart failure using SERCA2a gene therapy. Int J Mol Sci 2018;19:1086. doi: 10.3390/ijms19041086.
18. Netticadan T, Temsah R, Osada M, Dhalla NS. Status of Ca2+/calmodulin protein kinase phosphorylation of cardiac SR proteins in ischemia-reperfusion. Am J Physiol 1999;277:C384–C391. doi: 10.1152/ajpcell.1999.277.3.C384.
19. Zhai Y, Luo Y, Wu P, Li D. New insights into SERCA2a gene therapy in heart failure: Pay attention to the negative effects of B-type natriuretic peptides. J Med Genet 2018;55:287–296. doi: 10.1136/jmedgenet-2017-105120.
20. Zhang Y, Jiao L, Sun L, Li Y, Gao Y, Xu C, *et al*. LncRNA ZFAS1 as a SERCA2a inhibitor to cause intracellular Ca^{2+} overload and contractile dysfunction in a mouse model of myocardial infarction. Circ Res 2018;122:1354–1368. doi: 10.1161/circresaha.117.312117.

21. Mendler L, Braun T, Müller S. The ubiquitin-like SUMO system and heart function: From development to disease. Circ Res 2016; 118:132–144. doi: 10.1161/CIRCRESAHA.115.307730.
22. Chang HM, Yeh ETH. SUMO: From bench to bedside. Physiol Rev 2020;100:1599–1619. doi: 10.1152/physrev.00025.2019.
23. Kang J, Gocke CB, Yu H. Phosphorylation-facilitated SUMOylation of MEF2C negatively regulates its transcriptional activity. BMC Biochem 2006;7:5. doi: 10.1186/1471-2091-7-5.
24. Kho C, Lee A, Jeong D, Oh JG, Chaanine AH, Kizana E, *et al*. SUMO1-dependent modulation of SERCA2a in heart failure. Nature 2011;477:601–605. doi: 10.1038/nature10407.
25. Kho C, Lee A, Jeong D, Oh JG, Gorski PA, Fish K, *et al*. Small-molecule activation of SERCA2a SUMOylation for the treatment of heart failure. Nat Commun 2015;6:7229. doi: 10.1038/ncomms8229.
26. Du Y, Liu P, Xu T, Pan D, Zhu H, Zhai N, *et al*. Luteolin modulates SERCA2a leading to attenuation of myocardial ischemia/reperfusion injury via SUMOylation at lysine 585 in mice. Cell Physiol Biochem 2018;45:883–898. doi: 10.1159/000487283.
27. Tokarz P, Woźniak K. SENP proteases as potential targets for cancer therapy. Cancers (Basel) 2021;13:2059. doi: 10.3390/cancers13092059.
28. Hotz PW, Müller S, Mendler L. SUMO-specific isopeptidases tuning cardiac SUMOylation in health and disease. Front Mol Biosci 2021;8:786136. doi: 10.3389/fmolb.2021.786136.
29. Le NT, Martin JF, Fujiwara K, Abe JI. Sub-cellular localization specific SUMOylation in the heart. Biochim Biophys Acta Mol Basis Dis 2017;1863:2041–2055. doi: 10.1016/j.bbadis.2017.01.018.
30. Chen S, Dong D, Xin W, Zhou H. Progress in the discovery of small molecule modulators of deSUMOylation. Curr Issues Mol Biol 2020;35:17–34. doi: 10.21775/cimb.035.017.
31. Heo KS, Berk BC, Abe J. Disturbed flow-induced endothelial proatherogenic signaling via regulating post-translational modifications and epigenetic events. Antioxid Redox Signal 2016;25:435–450. doi: 10.1089/ars.2015.6556.
32. Gu J, Fan Y, Liu X, Zhou L, Cheng J, Cai R, *et al*. SENP1 protects against myocardial ischaemia/reperfusion injury via a HIF1α-dependent pathway. Cardiovasc Res 2014;104:83–92. doi: 10.1093/cvr/cvu177.
33. Hu F, Zhai N, Gao W, Wu P, Luo Y, Pan D, *et al*. Outer balloon ligation increases success rate of ischemia-reperfusion injury model in mice. PLoS One 2016;11:e0167631. doi: 10.1371/journal.pone.0167631.
34. Andersson KB, Finsen AV, Sjåland C, Winer LH, Sjaastad I, Odegaard A, *et al*. Mice carrying a conditional Serca2(flox) allele for the generation of Ca^{2+} handling-deficient mouse models. Cell Calcium 2009;46:219–225. doi: 10.1016/j.ceca.2009.07.004.
35. Doser TA, Turdi S, Thomas DP, Epstein PN, Li SY, Ren J. Transgenic overexpression of aldehyde dehydrogenase-2 rescues chronic alcohol intake-induced myocardial hypertrophy and contractile dysfunction. Circulation 2009;119:1941–1949. doi: 10.1161/CIRCULATIONAHA.108.823799.
36. Zhai K, Duan H, Wang W, Zhao S, Khan GJ, Wang M, *et al*. Ginsenoside Rg1 ameliorates blood-brain barrier disruption and traumatic brain injury via attenuating macrophages derived exosomes miR-21 release. Acta Pharm Sin B 2021;11:3493–3507. doi: 10.1016/j.apsb.2021.03.032.
37. Zhai KF, Zheng JR, Tang YM, Li F, Lv YN, Zhang YY, *et al*. The saponin D39 blocks dissociation of non-muscular myosin heavy chain IIA from TNF receptor 2, suppressing tissue factor expression and venous thrombosis. Br J Pharmacol 2017;174:2818–2831. doi: 10.1111/bph.13885.
38. Algoet M, Janssens S, Himmelreich U, Gsell W, Pusovnik M, Van den Eynde J, *et al*. Myocardial ischemia-reperfusion injury and the influence of inflammation. Trends Cardiovasc Med 2022; S1050-1738(22)00029-9. doi: 10.1016/j.tcm.2022.02.005.
39. Zhang RQ, Li DY, Xu TD, Zhu SS, Pan HJ, Fang F, *et al*. Antioxidative effect of luteolin pretreatment on simulated ischemia/reperfusion injury in cardiomyocyte and perfused rat heart. Chin J Integr Med 2017;23:518–527. doi: 10.1007/s11655-015-2296-x.
40. Qi L, Pan H, Li D, Fang F, Chen D, Sun H. Luteolin improves contractile function and attenuates apoptosis following ischemia-reperfusion in adult rat cardiomyocytes. Eur J Pharmacol 2011; 668:201–207. doi: 10.1016/j.ejphar.2011.06.020.
41. Luo Y, Shang P, Li D. Luteolin: A flavonoid that has multiple cardio-protective effects and its molecular mechanisms. Front Pharmacol 2017;8:692. doi: 10.3389/fphar.2017.00692.
42. Wu X, Xu T, Li D, Zhu S, Chen Q, Hu W, *et al*. ERK/PP1a/PLB/SERCA2a and JNK pathways are involved in luteolin-mediated protection of rat hearts and cardiomyocytes following ischemia/reperfusion. PLoS One 2013;8:e82957. doi: 10.1371/journal.pone.0082957.
43. Kawase Y, Ly HQ, Prunier F, Lebeche D, Shi Y, Jin H, *et al*. Reversal of cardiac dysfunction after long-term expression of SERCA2a by gene transfer in a pre-clinical model of heart failure. J Am Coll Cardiol 2008;51:1112–1119. doi: 10.1016/j.jacc.2007.12.014.
44. Torre E, Arici M, Lodrini AM, Ferrandi M, Barassi P, Hsu SC, *et al*. SERCA2a stimulation by istaroxime improves intracellular Ca2+ handling and diastolic dysfunction in a model of diabetic cardiomyopathy. Cardiovasc Res 2022;118:1020–1032. doi: 10.1093/cvr/cvab123.
45. Chen H, Liu S, Zhao C, Zong Z, Ma C, Qi G. Cardiac contractility modulation improves left ventricular systolic function partially via miR-25 mediated SERCA2A expression in rabbit trans aortic constriction heart failure model. J Thorac Dis 2018; 10:3899–3908. doi: 10.21037/jtd.2018.06.22.
46. Jiang Y, Tian LL, Wang LH, Zhao XD, Chen JW, Murao K, *et al*. Cardioprotective effects of Serca2a overexpression against ischemiareperfusion-induced injuries in rats. Curr Gene Ther 2017;17:248–258. doi: 10.2174/1566523217666171110175251.
47. Comerford KM, Leonard MO, Karhausen J, Carey R, Colgan SP, Taylor CT. Small ubiquitin-related modifier-1 modification mediates resolution of CREB-dependent responses to hypoxia. Proc Natl Acad Sci USA 2003;100:986–991. doi: 10.1073/pnas.0337412100.
48. Bae SH, Jeong JW, Park JA, Kim SH, Bae MK, Choi SJ, *et al*. SUMOylation increases HIF-1alpha stability and its transcriptional activity. Biochem Biophys Res Commun 2004;324:394–400. doi: 10.1016/j.bbrc.2004.09.068.
49. Albanese A, Daly LA, Mennerich D, Kietzmann T, Sée V. The role of hypoxia-inducible factor post-translational modifications in regulating its localisation, stability, and activity. Int J Mol Sci 2020;22:268. doi: 10.3390/ijms22010268.
50. Giorgino F, de Robertis O, Laviola L, Montrone C, Perrini S, McCowen KC, *et al*. The sentrin-conjugating enzyme mUbc9 interacts with GLUT4 and GLUT1 glucose transporters and regulates transporter levels in skeletal muscle cells. Proc Natl Acad Sci USA 2000;97:1125–1130. doi: 10.1073/pnas.97.3.1125.
51. Cimarosti H, Ashikaga E, Jaafari N, Dearden L, Rubin P, Wilkinson KA, *et al*. Enhanced SUMOylation and SENP-1 protein levels following oxygen and glucose deprivation in neurones. J Cereb Blood Flow Metab 2012;32:17–22. doi: 10.1038/jcbfm.2011.146.
52. Zhang H, Wang Y, Zhu A, Huang D, Deng S, Cheng J, *et al*. SUMO-specific protease 1 protects neurons from apoptotic death during transient brain ischemia/reperfusion. Cell Death Dis 2016; 7:e2484. doi: 10.1038/cddis.2016.290.
53. Cheng J, Kang X, Zhang S, Yeh ET. SUMO-specific protease 1 is essential for stabilization of HIF1alpha during hypoxia. Cell 2007;131:584–595. doi: 10.1016/j.cell.2007.08.045.
54. Xia Q, Mao M, Zeng Z, Luo Z, Zhao Y, Shi J, *et al*. Inhibition of SENP6 restrains cerebral ischemia-reperfusion injury by regulating Annexin-A1 nuclear translocation-associated neuronal apoptosis. Theranostics 2021;11:7450–7470. doi: 10.7150/thno.60277.

How to cite this article: Luo YY, Zhou SS, Xu T, Wu WL, Shang PP, Wang S, Pan DF, Li DY. SENP2-mediated SERCA2a deSUMOylation increases calcium overload in cardiomyocytes to aggravate myocardial ischemia/reperfusion injury. Chin Med J 2023;136:2496 –2507. doi: 10.1097/CM9.0000000000002757